Citation: Bucha B., Janák J. (2013) A MATLAB-based graphical user interface program for computing functionals of the geopotential up to ultra-high degrees and orders, *Computers & Geosciences* 56, 186–196, DOI: 10.1016/j.cageo.2013.03.012

A MATLAB-based graphical user interface program for computing functionals of the geopotential up to an arbitrary degree and order☆

Blažej Bucha[a,*], Juraj Janák[a]

[a]*Department of Theoretical Geodesy, Faculty of Civil Engineering, Slovak University of Technology in Bratislava, Radlinského 11, 813 68 Bratislava 15, Slovakia*

Abstract

We present a novel graphical user interface program GrafLab (GRAvity Field LABoratory) for spherical harmonic synthesis (SHS) created in MATLAB®. This program allows to comfortably compute 18 various functionals of the geopotential up to an arbitrary degree and order of spherical harmonic expansion. For the most difficult part of the SHS, namely the evaluation of the fully normalized associated Legendre functions (fnALFs), we used three different approaches according to required maximum degree: (i) the standard forward column method (up to maximum degree 1 800, in some cases up to degree 2 190); (ii) the modified forward column method combined with Horner's scheme (up to maximum degree 2 700); (iii) the extended-range arithmetic (up to an arbitrary maximum degree). For the maximum degree 2 190, the SHS with fnALFs evaluated using the extended-range arith-

☆Code available from `http://www.svf.stuba.sk/en/departments/department-of-theoretical-geodesy/science-and-research/downloads.html?page_id=4996`

*Corresponding author. Tel.: +421 2 59274342; fax: +421 2 52925476.

Email addresses: `blazej.bucha@stuba.sk` (Blažej Bucha), `juraj.janak@stuba.sk` (Juraj Janák)

metic approach takes only approximately 2-3 times longer than its standard arithmetic counterpart, i.e. the standard forward column method. In the GrafLab, the functionals of the geopotential can be evaluated on a regular grid or point-wise, while the input coordinates can either be read from a data file or entered manually. For the computation on a regular grid we decided to apply the lumped coefficients approach due to significant time-efficiency of this method. Furthermore, if a full variance-covariance matrix of spherical harmonic coefficients is available, it is possible to compute the commission errors of the functionals. When computing on a regular grid, the output functionals or their commission errors may be depicted on a map using automatically selected cartographic projection.
Keywords: Geopotential model, Gravity field functional, Spherical harmonic synthesis, Lumped coefficients, Commission error, Extended-range arithmetic

1. Introduction

In geodesy, the spherical harmonic expansion (SHE) is widely used for the determination of the Earth's external gravity field. The spherical harmonics provide an efficient mathematical tool for computing an arbitrary functional of the geopotential referred to a point lying on the Earth's surface or aloft; this process is known as the spherical harmonic synthesis (SHS). By definition, a functional is a special case of an operator, which associates to a function a real number (Moritz, 1980; Rektorys, 1999). The most common functionals of the geopotential are geoid undulation, height anomaly, gravity anomaly, gravity disturbance and deflections of the vertical. Nowadays,

the computation of these and many other functionals up to degree 2 190 is possible using the global geopotential model of the Earth (GGM) EGM2008 (Pavlis et al., 2012) and it can be expected that in the future the maximum degree of GGMs will continue to increase. However, hand in hand with the increasing degree of SHE, some numerical problems associated with the computation of spherical harmonics occur.

The principal problem in the computation of spherical harmonics of high degrees and orders is the numerical evaluation of associated Legendre functions of the first kind (ALFs) $P_{nm}(\cos\theta)$ (Hoffmann-Wellenhof and Moritz, 2005), which depend on the spherical co-latitude θ. Hence, ALFs are usually used in the fully normalized form (ibid.), which is algebraic method avoiding the numerical problems, so one obtains the fully normalized associated Legendre functions (fnALFs) $\overline{P}_{nm}(\cos\theta)$. However, for very high degrees and orders (e.g. 2 700), fnALFs still range over thousands of orders of magnitude and under-flow or over-flow problems occur (Holmes and Featherstone, 2002b). Some special care has to be put on the numerical evaluation of fnALFs. Thus, the standard recursive algorithms for computing values of fnALFs (cf. Colombo, 1981; Holmes and Featherstone, 2002b) have to be modified.

Holmes and Featherstone (2002b) presented an effective approach, which allows to compute fnALFs up to degree and order 2 700 for all co-latitudes without any under-flow or over-flow problems. This method is based on two factors: (i) eliminating the problematic term $\sin^m(\theta)$ from the recursions, so one obtains the scaled values of fnALFs $\overline{P}_{nm}(\cos\theta)/\sin^m(\theta)$; (ii) introducing a global scale factor of 10^{-280}. This two factors may be introduced into the

standard recursions obtaining the modified recursions, see e.g. Holmes and Featherstone (2002b). Once the scaled values of the fnALFs are obtained, the problematic term $\sin^m(\theta)$ is gradually re-introduced employing Horner's scheme and finally, after multiplication by the reciprocal value of the global scale factor, the non-scaled values of fnALFs are obtained.

These modified recursions are numerically stable up to the degree and order 2 700. For even higher degrees and orders, under-flow or over-flow problems occur again. Thus, this approach is also limited. Fukushima (2011) has introduced another approach, which enables to compute fnALFs up to extremely high degree such as $2^{32} = 4\ 294\ 967\ 296$, by modifying the idea of extended-range arithmetic (Smith et al., 1981). In extended-range arithmetic, a non-zero arbitrary real number X is expressed as $X = x\,B^{i_X}$, where B is the radix (a large power of 2), x is the significand and i_X is the exponent. Another words, a separate storage location to the exponent of each floating-point number is allocated (Wittwer et al., 2008). In the double-precision Fukushima (2011) used the radix value $B = 2^{960}$. Hence, much bigger and smaller numbers can be represented in the IEEE (Institute of Electrical and Electronic Engineers') double-precision, so fnALFs of an arbitrary degree and order can be evaluated using the standard recursions without an under-flow problem. For more details about the extended-range arithmetic, the reader is advised to Fukushima (2011) or Smith et al. (1981).

Several computer programs for evaluating various functionals of the geopotential have been developed so far, e.g. Holmes and Pavlis (2008); Janák and Šprlák (2006); Sanso and Sona (2001); Smith (1998); Tscherning et al. (1983); Wittwer et al. (2008). However, most of them, except Wittwer et al. (2008),

are restricted to a certain maximum degree of SHE (e.g. 2 700). In this paper, we present the novel MATLAB®-based graphical user interface (GUI) program for computing functionals of the geopotential up to an arbitrary degree and order. The outline of the paper is as follows: in section 2, the accuracy tests for the numerical evaluation of fnALFs using the three above mentioned approaches (i.e. the standard recursions, the modified recursions combined with Horner's scheme and the extended-range arithmetic) are introduced. The SHS process, the lumped coefficients approach and the error propagation are described in this section as well. The developed software GrafLab and the numerical tests are introduced in section 3. In section 4, the contributions of the designed software and summary are presented.

2. Spherical harmonic synthesis

Let us start with the basic and well-known formula for the Earth's external gravitational potential, expressed in the truncated series of the spherical harmonics (Hoffmann-Wellenhof and Moritz, 2005)

$$V(r,\theta,\lambda) = \frac{GM}{r} + \frac{GM}{r}\sum_{n=2}^{M}\left(\frac{R}{r}\right)^{n}\sum_{m=0}^{n}\big(\overline{C}_{nm}\,\cos m\lambda + \overline{S}_{nm}\,\sin m\lambda\big)\,\overline{P}_{nm}(\cos\theta), \tag{1}$$

in which GM is the geocentric gravitational constant of the Earth, R is the radius of the Earth, (r,θ,λ) is the triplet of the spherical coordinates (spherical radius, spherical co-latitude and spherical longitude, respectively), $\overline{P}_{nm}(\cos\theta)$ are the fnALFs of degree n and order m, $\overline{C}_{nm}$ and $\overline{S}_{nm}$ are the fully normalized spherical harmonic coefficients of degree n and order m and M is the maximum degree of the SHE. Eq. (1) may be written in the form

of inverted summations over n and m as

$$V(r,\theta,\lambda) = \frac{GM}{r} + \frac{GM}{r}\sum_{m=0}^{M}\left[\cos m\lambda \sum_{n=\mu}^{M}\left(\frac{R}{r}\right)^{n} \overline{C}_{nm}\,\overline{P}_{nm}(\cos\theta) + \sin m\lambda \sum_{n=\mu}^{M}\left(\frac{R}{r}\right)^{n} \overline{S}_{nm}\,\overline{P}_{nm}(\cos\theta)\right], \tag{2}$$

where μ is either 2 or m, whichever is the greater. If the fixed-degree recursions have been used to compute fnALFs, Eq. (1) is more suitable, while Eq. (2) should be used with the fixed-order recursions. In geodesy, Eq. (2) and fixed-order recursions are usually preferred rather than Eq. (1) and fixed-degree recursions.

In fact, Eq. (1) as well as Eq. (2) can be considered as the basic formulae of SHS, from which an arbitrary functional of the geopotential can be derived, see e.g. Barthelmes (2009).

2.1. Numerical computation of the fully normalized associated Legendre functions and their first- and second-order derivatives

The numerical evaluation of fnALFs and their derivatives up to a high degree is the most difficult part of the SHS. In the GrafLab, we used three different approaches, which have been mentioned in section 1: (i) the standard forward column method (Holmes and Featherstone, 2002b); (ii) the modified forward column method (ibid.); (iii) the extended-range arithmetic (Fukushima, 2011). It is not the purpose of this paper to recapitulate here recursions that can be found in many literature (Bosch, 2000; Colombo, 1981; Fantino and Casotto, 2009; Fukushima, 2011, 2012; Holmes and Featherstone, 2002a,b). However, it should be mentioned that these recursions can

be modified by introducing the term $(R/r)^n$ so that we finally get

$$\widetilde{P}_{nm}(\cos\theta) = \left(\frac{R}{r}\right)^n \overline{P}_{nm}(\cos\theta), \tag{3}$$

which we name the modified fnALF. The main reason for doing this is that the modified fnALFs may be evaluated directly during the recursions and thus reduced the computation time of the whole SHS process, since large matrix multiplications are eliminated. The reader can find more about this approach e.g. in Bethencourt et al. (2005). In this section, we will focus on the numerical stability of the recurrence relations used up to high and ultra-high degrees. For this tests, the ordinary fnALFs instead of the modified fnALFs were used.

In order to verify the numerical accuracy of computed fnALFs and their derivatives, we used the accuracy test presented in Holmes and Featherstone (2002b). Independently on the co-latitude, the following formulae must hold (Fukushima, 2011, 2012)

$$I^{(0)} = \sum_{n=0}^{M}\sum_{m=0}^{n}\left(\overline{P}^{(0)}_{nm}(\cos\theta)\right)^2 = (M+1)^2, \quad \forall\theta, \tag{4a}$$

$$I^{(1)} = \sum_{n=0}^{M}\sum_{m=0}^{n}\left(\overline{P}^{(1)}_{nm}(\cos\theta)\right)^2 = \frac{M(M+2)(M+1)^2}{4}, \quad \forall\theta, \tag{4b}$$

$$I^{(2)} = \sum_{n=0}^{M}\sum_{m=0}^{n}\left(\overline{P}^{(2)}_{nm}(\cos\theta)\right)^2 = \left(\frac{M^2+2M-1}{2}\right) I^{(1)}, \quad \forall\theta, \tag{4c}$$

wherein $\overline{P}^{(0)}_{nm}(\cos\theta)$, $\overline{P}^{(1)}_{nm}(\cos\theta)$ and $\overline{P}^{(2)}_{nm}(\cos\theta)$ denote the zero-, first- and second-order derivatives of fnALFs with respect to the spherical co-latitude, respectively. The identity error is then given as

$$\delta I^{(d)} = \left| \frac{I^{(d)}_{\text{computed}}}{I^{(d)}_{\text{theoretical}}} - 1 \right|, \tag{5}$$

where $d = 0, 1, 2$ denotes the order of the derivatives of fnALFs. Note that in the case of the modified forward column method, the scaled values of fnALFs or their derivatives must be combined with Horner's scheme, see Holmes and Featherstone (2002b).

The values of $\overline{P}_{nm}^{(d)}(\cos\theta)$ range over thousands of orders of magnitude and therefore cannot be squared (see Eqs. (4a)-(4c)) in double precision due to the under-flow and over-flow problems. Hence, these values were computed in double precision using the above mentioned approaches, subsequently they were converted to quadruple precision and finally, squared and summed in quadruple precision. However, MATLAB® does not support the quadruple precision, thus, these algorithms were rewritten into Fortran 90, compiled by the Intel Visual Fortran Composer XE 2011 and executed at a computer with 2.5 GHz dual-core CPU and 3 GB RAM under the 32 bit Windows 7 OS. The routines used for computing fnALFs using the extended-range arithmetic, written in Fortran 90, are available from Fukushima (2011). These routines were rewritten into the MATLAB® and used in the GrafLab software.

Based on our numerical accuracy tests, the three above mentioned approaches may be used up to the following maximum degrees:

(i) the standard forward column method: $M_{\max} = 1\ 800$,

(ii) the modified forward column method: $M_{\max} = 2\ 700$,

(iii) the extended-range arithmetic: up to an arbitrary degree.

These statements are supported by Figures A.1 - A.3, which represent the base-10 logarithm of the identity errors $\delta I^{(d)}$ computed for all integer values of co-latitudes $0^\circ \leq \theta \leq 90^\circ$ in the case of $d = 0$ and $0^\circ < \theta \leq 90^\circ$ if $d = 1, 2$. Note that the recurrence relations used for evaluating the first- and

second-order derivatives of fnALFs are singular at poles (Fukushima, 2012, Appendix A.1).

Figure A.1 should be positioned here

Figure A.2 should be positioned here

Figure A.3 should be positioned here

Furthermore, inspection of Figure A.4 shows that the standard forward column method may also be used up to degree $M = 2\,190$, but only for the co-latitudes $\theta \in \langle 0°, 10° \rangle \cup \langle 34°, 90° \rangle$ in the case of fnALFs and $\theta \in (0°, 10°\rangle \cup \langle 34°, 90° \rangle$ in the case of their derivatives. The computational labor of this approach is the lowest, therefore this approach should be applied if possible. We will focus on the time-efficiency of these three approaches in section 3.2.

Figure A.4 should be positioned here

2.2. Lumped coefficients approach

When applying Eq. (2) on a regular grid, it may be rewritten into a much efficient form. Both summation, i.e. the summation over n and subsequently over m, can be done by matrix multiplications using the lumped coefficients, sometimes called the Fourier coefficients. In Eq. (2), the terms $\sum_{n=\mu}^{M} (R/r)^n \, \overline{C}_{nm} \, \overline{P}_{nm}(\cos\theta)$ and $\sum_{n=\mu}^{M} (R/r)^n \, \overline{S}_{nm} \, \overline{P}_{nm}(\cos\theta)$ are constant for each meridian in the grid and therefore no need to be computed more than once. With this in mind, Eq. (2) may be written in the matrix form as

$$\mathbf{V} = (GM \oslash \mathbf{r}) \odot \left[1 + \Big(\mathbf{A}(\boldsymbol{\theta}) \cdot \cos(\mathbf{m} \cdot \boldsymbol{\lambda}) + \mathbf{B}(\boldsymbol{\theta}) \cdot \sin(\mathbf{m} \cdot \boldsymbol{\lambda}) \Big) \right], \qquad (6)$$

in which $\mathbf{A}_{N_\theta\times(M+1)}(\boldsymbol{\theta})$ and $\mathbf{B}_{N_\theta\times(M+1)}(\boldsymbol{\theta})$ are the matrices of the lumped coefficients, where N_θ denotes the number of the points in one meridian, $\mathbf{r}_{N_\theta\times N_\lambda}$ is the matrix of the spherical radii of every point in the grid, N_λ denotes the number of the points in one latitude parallel, $\boldsymbol{\theta}_{N_\theta\times 1}$ is the column vector of the spherical co-latitudes, $\boldsymbol{\lambda}_{1\times N_\lambda}$ is the row vector of the spherical longitudes and $\mathbf{m}_{(M+1)\times 1}$ is the column vector with the structure $\mathbf{m} = \begin{bmatrix} 0 & 1 & \dots & M \end{bmatrix}^\top$. The symbol $\odot$ denotes the Hadamard product (Grafarend, 2006), which may be used for the matrices of the same dimensions in order to multiply each corresponding elements of the matrices (element-wise product), while the symbol $\cdot$ denotes the Cayley product (matrix product) (ibid.). We also introduced the symbol $\oslash$, which denotes an element-wise division of a scalar (or a matrix) by a matrix. In fact, in Eq. (6) only the vector $\mathbf{r}_{N_\theta\times 1}$ is needed instead of the matrix $\mathbf{r}_{N_\theta\times N_\lambda}$, and each column of the matrix in the square brackets in Eq. (6) may be multiplied using the Hadamard product by the vector $\mathbf{r}_{N_\theta\times 1}$, so there is no need to store the redundant data. In MATLAB®, the built-in function bsxfun® is designed for this purpose. However, for the sake of clarity we used this notation in the whole paper, but in the GrafLab, the bsxfun® function was used.

The vectors of the lumped coefficients of order m are defined as

$$\left.\begin{matrix} \mathbf{A}_m(\boldsymbol{\theta}) \\ \mathbf{B}_m(\boldsymbol{\theta}) \end{matrix}\right\} = \widetilde{\mathbf{P}}_m \cdot \begin{Bmatrix} \overline{\mathbf{C}}_m \\ \overline{\mathbf{S}}_m \end{Bmatrix} \tag{7}$$

where $\widetilde{\mathbf{P}}_m$ is the matrix of the modified fnALFs with the structure

$$\widetilde{\mathbf{P}}_m = \begin{bmatrix} \widetilde{P}_{m,m}(\cos\theta_1) & \widetilde{P}_{m+1,m}(\cos\theta_1) & \cdots & \widetilde{P}_{M,m}(\cos\theta_1) \\ \widetilde{P}_{m,m}(\cos\theta_2) & \widetilde{P}_{m+1,m}(\cos\theta_2) & \cdots & \widetilde{P}_{M,m}(\cos\theta_2) \\ \vdots & \vdots & \ddots & \vdots \\ \widetilde{P}_{m,m}(\cos\theta_{N_\theta}) & \widetilde{P}_{m+1,m}(\cos\theta_{N_\theta}) & \cdots & \widetilde{P}_{M,m}(\cos\theta_{N_\theta}) \end{bmatrix} \tag{8}$$

and

$$\overline{\mathbf{C}}_m = \begin{bmatrix} \overline{C}_{m,m} & \overline{C}_{m+1,m} & \cdots & \overline{C}_{M,m} \end{bmatrix}^\top, \tag{9a}$$

$$\overline{\mathbf{S}}_m = \begin{bmatrix} \overline{S}_{m,m} & \overline{S}_{m+1,m} & \cdots & \overline{S}_{M,m} \end{bmatrix}^\top. \tag{9b}$$

Finally, we obtain the full matrices of the lumped coefficients

$$\mathbf{A}(\boldsymbol{\theta}) = \begin{bmatrix} \mathbf{A}_{m=0}(\boldsymbol{\theta}) & \mathbf{A}_{m=1}(\boldsymbol{\theta}) & \cdots & \mathbf{A}_{m=M}(\boldsymbol{\theta}) \end{bmatrix}, \tag{10a}$$

$$\mathbf{B}(\boldsymbol{\theta}) = \begin{bmatrix} \mathbf{B}_{m=0}(\boldsymbol{\theta}) & \mathbf{B}_{m=1}(\boldsymbol{\theta}) & \cdots & \mathbf{B}_{m=M}(\boldsymbol{\theta}) \end{bmatrix}. \tag{10b}$$

Using this approach, an arbitrary functional of the geopotential can be evaluated on a regular grid much faster than using the point-wise approach with two loops, one degree-depended and one order-depended. In fact, the factor of increased computational speed is of several thousands, which is remarkable.

2.3. Error propagation

In general, the spherical harmonic coefficients are estimated by the least squares method using terrestrial and/or satellite measurements, which are not errorless. The least squares method enables to estimate the full variance-covariance matrix of these coefficients as well. When computing an arbitrary

functional of the geopotential using these estimated coefficients, their errors are propagated to the functional obeying the error variance-covariance propagation law (Grafarend, 2006). This error is known as the commission error. For the linear transformation of the variance-covariance matrix of the spherical harmonic coefficients to the variance-covariance matrix of the gravitational potential the following formula may be written

$$\mathbf{\Sigma_V} = \mathbf{A} \cdot \mathbf{\Sigma_{SHC}} \cdot \mathbf{A}^\top, \tag{11}$$

where $\mathbf{\Sigma_{SHC}}$ is the variance-covariance matrix of the spherical harmonic coefficients with the structure

$$\mathbf{\Sigma_{SHC}} = \begin{bmatrix} v^{CC}_{20,20} & c^{CC}_{20,30} & \cdots & c^{CC}_{20,M0} & c^{CC}_{20,21} & c^{CS}_{20,21} & c^{CC}_{20,31} & \cdots & c^{CS}_{20,MM} \\ c^{CC}_{30,20} & v^{CC}_{30,30} & \cdots & c^{CC}_{30,M0} & c^{CC}_{30,21} & c^{CS}_{30,21} & c^{CC}_{30,31} & \cdots & c^{CS}_{30,MM} \\ \vdots & \vdots & \ddots & \vdots & \vdots & \vdots & \vdots & \cdots & \vdots \\ c^{CC}_{M0,20} & c^{CC}_{M0,30} & \cdots & v^{CC}_{M0,M0} & c^{CC}_{M0,21} & c^{CS}_{M0,21} & c^{CC}_{M0,31} & \cdots & c^{CS}_{M0,MM} \\ c^{CC}_{21,20} & c^{CC}_{21,30} & \cdots & c^{CC}_{21,M0} & v^{CC}_{21,21} & v^{CS}_{21,21} & v^{CC}_{21,31} & \cdots & v^{CS}_{21,MM} \\ c^{SC}_{21,20} & c^{SC}_{21,30} & \cdots & c^{SC}_{21,M0} & c^{SC}_{21,21} & v^{SS}_{21,21} & v^{SC}_{21,31} & \cdots & v^{SS}_{21,MM} \\ c^{CC}_{31,20} & c^{CC}_{31,30} & \cdots & c^{CC}_{31,M0} & c^{CC}_{31,21} & c^{CS}_{31,21} & v^{CC}_{31,31} & \cdots & c^{CS}_{31,MM} \\ \vdots & \vdots & \cdots & \vdots & \vdots & \vdots & \vdots & \ddots & \vdots \\ c^{SC}_{MM,20} & c^{SC}_{MM,30} & \cdots & c^{SC}_{MM,M0} & c^{SC}_{MM,21} & c^{SS}_{MM,21} & c^{SC}_{MM,31} & \cdots & v^{SS}_{MM,MM} \end{bmatrix}, \tag{12}$$

where $v^{CC}_{20,20}$ denotes the variance of the coefficient $\overline{C}_{20}$, $c^{CS}_{20,21}$ is the covariance between the coefficients $\overline{C}_{20}$ and $\overline{S}_{21}$, etc., and $\mathbf{A}$ is the design matrix of the partial derivatives of Eq. (2) with respect to the individual spherical harmonic coefficients. Note that the partial derivatives in the matrix $\mathbf{A}$ must correspond to the organization of the individual elements in the matrix $\mathbf{\Sigma_{SHC}}$. Since the structure of the matrix $\mathbf{\Sigma_{SHC}}$ has not yet been standardized, only this particular structure of the variance-covariance matrix, which is probably the most common, can be recognized by the GrafLab. Finally, the square

roots of the diagonal elements of the matrix $\mathbf{\Sigma_V}$ represent the commission errors of the gravitational potential in the particular computing points.

Note that the matrix $\mathbf{\Sigma_{SHC}}$ of a GGM may or may not be calibrated. If the matrix $\mathbf{\Sigma_{SHC}}$ is calibrated, the computed commission errors may be considered as real. If this matrix is not calibrated, the evaluated commission errors must be considered only as a relative indicator of accuracy of the GGM in a certain area on the globe with respect to another area.

3. Software presentations

3.1. Description of the software

In this section, we will describe in detail the created software GrafLab (GRAvity Field LABoratory) and the basic principles of manipulation with the software. The source code of the GrafLab, as well as its graphical user interface (GUI), have been written in MATLAB®. The GUI, see Figure A.5, allows comfortable and intuitive manipulation with all functionalities of the software.

Figure A.5 should be positioned here

The GUI of the application is visually divided into three panels:

(i) *Geopotential model and reference system selection*: At first, the input GGM file or its error variance-covariance matrix must be imported using the *Browse...* button. The input GGM file must have one of the two standardized structures, see Table A.1 and Table A.2. Only this two structures can be recognized by the GrafLab. In addition to the spherical harmonic coefficients, the input file may or may not contains the fifth and the sixth column

with their standard deviations. The input file may either be an ASCII file or a binary MAT-file. In case of the GGM with a high maximum degree of SHE, it is recommended to use the binary MAT-file, since it can be loaded much faster.

Table A.1 should be positioned here

Table A.2 should be positioned here

The input ASCII file of error variance-covariance matrix must have the structure as shown in the Table A.3. A binary MAT-file may be used to import error variance-covariance matrix as well. However, in this case, the empty arrays in Table A.3 must be filled with zeroes or corresponding covariances.

Table A.3 should be positioned here

Most of GGMs have the same values of the geocentric gravitational constant and the radius of the Earth, therefore in this panel GrafLab automatically offers these values for the computation. However, they may be simply replaced by the required values, if necessary. The $n_{\min}$ value of SHE is implicitly set to 2 and cannot be changed, unlike the value of $n_{\max}$. Only integer values of $n_{\max}$ in the interval $n_{\max} \in \langle 2, M \rangle$ are accepted. From the pop-up menu *Ellipsoid*, the normal gravity field generated by the equipotential ellipsoid WGS84 (NIMA, 2000) or GRS80 (Moritz, 2000) can be selected.

(ii) *Point type selection*: In the point type selection panel, one of three organizations of the evaluation points must be specified by selecting the check-box: *Grid*, *Load data* or *Point-wise*. If the grid is selected, the minimum,

maximum and discretization step in the ellipsoidal latitude and ellipsoidal longitude directions must be entered. The array *h (m)* denotes the constant ellipsoidal height of the grid above the reference ellipsoid. For the computation on a regular grid, the lumped coefficients approach described in section 2.2 is used.

To import the computational points from a data file, the *Load data* checkbox must be selected and subsequently, the data file must be imported using the *Browse...* button next to the checkbox. The data file may contain essentially an arbitrary number of lines and in every line of the file, the triplet of the ellipsoidal coordinates (ellipsoidal latitude, ellipsoidal longitude and ellipsoidal height) must be given.

After selecting the checkbox *Point-wise*, an arbitrary point defined also by the triplet of the ellipsoidal coordinates can be entered manually using the arrays *phi (°)*, *lambda (°)*, *h (m)*. In case of several points, the coordinates in each array must be separated by the comma or by the space. This point type selection is suitable if only a few points are to be determined, so there is no need to create a data file to import.

In the last two mentioned cases of the point type selection, the lumped coefficients approach cannot be applied due to irregular distribution of the points. Therefore we used two loops, one degree-depended and one order-depended, and programmed the routines for computing all functionals as it is shown in Eq. (2).

In each of the three above mentioned point type selections, the entries must be either in the form of floating point numbers with decimal dots or integer values.

(iii) *Calculated parameters and output selection*: Using the four pop-up menus on the left side of this panel, user can simply choose, which functionals of the geopotential are to be computed. Note that at least one and maximum four functionals may be computed simultaneously. GrafLab permits to compute the following functionals of the geopotential (the value in the superscript denotes the level of computational demand; (1) is small, (2) is medium and (3) is high): gravitational potential $V^{(1)}$, diagonal components of the gravitational tensor in the spherical coordinates $V_{rr}^{(3)}, V_{\theta\theta}^{(3)}, V_{\lambda\lambda}^{(3)}$, non-diagonal components of the gravitational tensor in the spherical coordinates $V_{r\theta}^{(3)}, V_{r\lambda}^{(3)}, V_{\theta\lambda}^{(3)}$, diagonal components of the gravitational tensor in the local north-oriented frame (LNOF) $V_{xx}^{(2)}, V_{yy}^{(2)}, V_{zz}^{(2)}$, non-diagonal components of the gravitational tensor in the LNOF $V_{xy}^{(3)}, V_{xz}^{(3)}, V_{yz}^{(3)}$, gravity potential $W^{(1)}$, gravity $g^{(2)}$, gravity in spherical approximation $g_{sa}^{(1)}$, second radial derivative of gravity potential $W_{rr}^{(1)}$, disturbing potential $T^{(1)}$, gravity disturbance $\delta g^{(2)}$, gravity disturbance in spherical approximation $\delta g_{sa}^{(1)}$, gravity anomaly in spherical approximation $\Delta g_{sa}^{(1)}$, second radial derivative of disturbing potential $T_{rr}^{(1)}$, diagonal components of the disturbing tensor in the spherical coordinates $T_{rr}^{(3)}, T_{\theta\theta}^{(3)}, T_{\lambda\lambda}^{(3)}$, non-diagonal components of the disturbing tensor in the spherical coordinates $T_{r\theta}^{(3)}, T_{r\lambda}^{(3)}, T_{\theta\lambda}^{(3)}$, diagonal components of the disturbing tensor in the LNOF $T_{xx}^{(2)}, T_{yy}^{(2)}, T_{zz}^{(2)}$, non-diagonal components of the disturbing tensor in the LNOF $T_{xy}^{(3)}, T_{xz}^{(3)}, T_{yz}^{(3)}$, north-south component of the deflection of the vertical $\xi^{(2)}$, east-west component of the deflection of the vertical $\eta^{(1)}$, total deflection of the vertical $\Theta^{(2)}$, geoid undulation $N^{(2)}$, generalized height anomaly $\zeta_{Ell}^{(1)}$, height anomaly $\zeta^{(2)}$. In order to stay brief, we do not introduce here the mathematical formulae for

computing each functional, but these can be found in the pdf file Definition_of_functionals_of_the_geopotential_used_in_GrafLab_software.pdf available at [1]. For evaluating disturbing and gravitational tensor in the LNOF, we used the non-singular expressions, which can be found e.g. in Petrovskaya and Vershkov (2006). For practical reasons, we slightly modified these formulae, see Appendix A.

To compute geoid undulation N and height anomaly ζ, the digital terrain model, e.g. DTM2006.0 (Pavlis et al., 2007), must be imported. Only one particular structure of the DTM file, shown in Table A.1, can be recognized by the GrafLab. If these two functionals are to be computed, immediately after clicking the *OK* button, the dialog window from which the input DTM file must be imported will appear.

Each functional of the geopotential may be evaluated using any of the three mentioned approaches for computing fnALFs except for the gravitational and disturbing tensors in the LNOF. Since these non-singular expressions have been slightly modified, the modified forward column method combined with Horner's scheme is not efficient for the new formulae and therefore it was not used in this case.

In order to evaluate the commission errors of the functionals, the *Commission error* check box must be selected. GrafLab allows to compute the commission errors (see section 2.3) of the each above mentioned functional except for the gravitational and disturbing tensors in the LNOF: T_{xx}, T_{yy}, T_{zz}; T_{xy}, T_{xz}, T_{yz}; V_{xx}, V_{yy}, V_{zz}; V_{xy}, V_{xz}, V_{yz}. One should keep in mind that the

[1] `http://www.svf.stuba.sk/en/departments/department-of-theoretical-geodesy/science-and-research/downloads.html?page_id=4996`

evaluation of commission error has much higher requirements on the computer, because of the large size of the matrix $\mathbf{\Sigma_{SHC}}$. In practice it means that the maximum degree M must be reduced from thousands or hundreds to tens, and number of computing points have to be decreased as well.

By clicking the button *Computation of fnALFs*, a new dialog window will appear, see Figure A.6, in which user may choose one of the three approaches for evaluating values of fnALFs (see section 2.1).

Figure A.6 should be positioned here

The computed data may be depicted on a map using automatically selected cartographic projection. By clicking the button *Display data settings*, another dialog window illustrated by Figure A.7 will appear. Here, user can set up the required output parameters of the exported map. This option is available only if the computation on a regular grid has been chosen. Demonstrations of exported maps are shown in Figure A.8 and Figure A.9.

Figure A.7 should be positioned here

Figure A.8 should be positioned here

Figure A.9 should be positioned here

The button *Output folder and file* permits to specify the output folder and prefix of the all exported files, i.e. without any suffix (e.g. Prefix). The data file (e.g. Prefix.txt) with the computed data may be created by selecting the checkbox *Export data*. The report file, which contains the informations about the computation, see Table A.4, may be created by selecting

the *Export report* checkbox. This file automatically obtains name with the suffix _Report.txt, e.g. Prefix_Report.txt. If the *Display data* checkbox has been selected, GrafLab creates also a graphical file (or files, depending on the number of computing functionals) according to chosen graphic file format (bmp, emf, eps, jpeg, pdf, png or tiff).

Table A.4 should be positioned here

When all the required input parameters and input files have been entered, after clicking the *OK* button, the computation will start. On the left from this button, there is a status line, which provides short explanations during the whole computational process (*Loading GGM file...*, current value of the variable m in the order-dependent loop, *Displaying data...*, ...), so one can clearly see in which part of the computation is GrafLab. After successful computation, the status *Computation has been finished* will appear. If any of the input parameters or input files have been entered in a wrong format, GrafLab will open a warning dialog or error dialog with description of the error.

The whole source code of the program called GrafLab.m is written as a one function. It contains approximately 8 000 lines of the source code, therefore in Figure A.10 we provide a simple flowchart of the program, so one can clearly see its structure.

Figure A.10 should be positioned here

3.2. Testing of the software

In this section, we focus on the efficiency of the algorithms used in the GrafLab. We performed two separate tests, one for the lumped coefficients approach (computation on a regular grid) and the second for the point-wise approach (computation on irregularly distributed points). In each experiment we tested the time-efficiency of all three approaches for computing values of fnALFs in the context of SHS. For these tests we chose two functionals: disturbing potential and disturbing tensor in the LNOF (diagonal and off-diagonal elements separately). All numerical experiments were performed on an ordinary computer with 2.5 GHz dual-core CPU and 3 GB RAM under the 32 bit Windows 7 OS.

In Figure A.11 and Figure A.12 we plot the CPU time for computing disturbing potential using $M = 360$ and $M = 2\ 190$, respectively, on a global grid versus different grid resolution. The same numerical tests using disturbing tensor are illustrated in Figure A.13 and Figure A.14. Note that the standard forward column method should not be applied on a global grid if $M > 1\ 800$, see Figure A.4. However, in order to assess the time-efficiency of the algorithm only, it was used.

Figure A.11 should be positioned here

Figure A.12 should be positioned here

Figure A.13 should be positioned here

Figure A.14 should be positioned here

Figure A.13 and Figure A.14 reveal that all gravity gradients in the LNOF

(i.e. diagonal and off-diagonal elements of the tensor) can be synthesized on a global grid $5' \times 5'$ within 74 s if $M = 360$ and on a global grid $10' \times 10'$ within 936 s if $M = 2\ 190$.

Similar tests, see Figures A.15 - A.18, were done for the point-wise approach, in which we used the computational points randomly distributed on the globe.

Figure A.15 should be positioned here

Figure A.16 should be positioned here

Figure A.17 should be positioned here

Figure A.18 should be positioned here

As expected, the point-wise approach is significantly more time-consuming than the lumped coefficients approach. Hence, for a high maximum degree (e.g. $M = 2\ 190$) we recommend to use this approach for tens of thousands of computation points at most.

In general, from Figures A.11 - A.18 it is seen that the SHS with fnALFs evaluated using the extended-range arithmetic takes only approximately 2-3 times longer than using the standard forward column method. Furthermore, for a large data set on a grid and maximum degrees ranging from 1 801 to 2 700, it is much more effective to use the extended-range arithmetic than the modified forward column method. In contrast, in the point-wise approach and maximum degrees in the same interval, the modified forward column method should be preferred rather than the extended-range arithmetic, since it required significantly less computation time.

As mentioned, the tests were performed on a 32 bit version of MATLAB® and Windows 7 OS. However, on a 64 bit architecture we found the algorithm for computing fnALFs using extended-range arithmetic extremely slow. Thus, to make this algorithm more effective on this architecture, we slightly modified the program in order to speed up the extended-range arithmetic approach. However, on a 64 bit version of MATLAB® the extended-range arithmetic approach still remains 8-10 times slower than the standard forward column method. During the computation, GrafLab automatically identifies the bit architecture of MATLAB® on which the computation is performed and uses the appropriate version of the algorithm.

4. Summary

In this paper, we have been presented a new MATLAB®-based graphical user interface program for spherical harmonic synthesis. GrafLab allows to easily compute and depict 18 various functionals of the geopotential as well as their commission errors. Fully normalized ALFs may be obtained using three different approaches from which one approach enables to evaluate the fnALFs up to an arbitrary degree and order in the cost of only 2-3 times increased computation time compared with the standard algorithms. A modified non-singular expressions for the gravity gradients in the LNOF have been introduced as well.

The main advantages of the GrafLab are that it is not restricted to a maximum degree of SHE essentially, it is fast, versatile and simple for usage through an intuitive and comfortable GUI. The primary exploitation of the GrafLab is supposed to be in scientific tasks related to the spherical harmonic

synthesis of functionals of the geopotential. Since the program is controlled through a convenient GUI, it may be used as an efficient tool for educational purposes as well.

Acknowledgements

The work has been supported by the national projects VEGA 1/1092/11 and APVV-0072-11. The authors are thankfull to the anonymous referees for their valuable comments, which improved the quality of the original manuscript.

Appendix A. Modified non-singular expressions for the gravity gradients in the LNOF

The used non-singular expressions for the gravity gradients in the LNOF can be found e.g. in Petrovskaya and Vershkov (2006). We will not recapitulate here all those formulae. As an example, let us mentioned only one particular expression for the element T_{xx}, which has the following form

$$\begin{aligned} T_{xx} =& \frac{GM}{r^3} \sum_{n=2}^{M} \left(\frac{R}{r}\right)^n \sum_{m=0}^{n} \left(\overline{C}_{nm} \cos m\lambda + \overline{S}_{nm} \sin m\lambda\right) \\ & \times \Big(a_{nm}\, \overline{P}_{n,m-2}(\cos\theta) \\ & + \left[b_{nm} - (n+1)(n+2)\right] \overline{P}_{nm}(\cos\theta) \\ & + c_{nm}\, \overline{P}_{n,m+2}(\cos\theta) \Big), \end{aligned} \tag{A.1}$$

in which

$$a_{nm} = 0, \quad m = 0, 1 \tag{A.2}$$

$$a_{nm} = \frac{\sqrt{1+\delta_{m,2}}}{4}\sqrt{n^2-(m-1)^2} \times \sqrt{n+m}\sqrt{n-m+2}, \quad 2 \le m \le n \tag{A.3}$$

$$b_{nm} = \frac{(n+m+1)(n+m+2)}{2\,(m+1)}, \quad m = 0, 1 \tag{A.4}$$

$$b_{nm} = \frac{n^2+m^2+3n+2}{2}, \quad 2 \le m \le n \tag{A.5}$$

$$c_{nm} = \frac{\sqrt{1+\delta_{m,0}}}{4}\sqrt{n^2-(m+1)^2}\sqrt{n-m} \times \sqrt{n+m+2}, \quad m = 0, 1 \tag{A.6}$$

$$c_{nm} = \frac{1}{4}\sqrt{n^2-(m+1)^2}\sqrt{n-m}\sqrt{n+m+2}, \quad 2 \le m \le n \tag{A.7}$$

$$\delta_{p,q} = \begin{cases} 1, & p = q, \\ 0, & p \ne q. \end{cases} \tag{A.8}$$

From Eq. (A.1), one can see that in addition to the term $\overline{P}_{nm}(\cos\theta)$, two other terms $\overline{P}_{n,m-2}(\cos\theta)$ and $\overline{P}_{n,m+2}(\cos\theta)$ must be computed for each m. From the practical numerical point of view, this is not an issue, if fixed-degree recursions have been used to evaluate fnALFs. In this case, for each m these terms have been already computed with the term $\overline{P}_{nm}(\cos\theta)$ essentially. In the GrafLab, however, we used fixed-order recursions, which are preferred in geodesy. In this case, with every change of m in the order-dependent loop, it is necessary to evaluate not only the term $\overline{P}_{nm}(\cos\theta)$, but also the two other terms. Another words, redundant computations occur. Thus, we modified Eq. (A.1) in the way that only the term $\overline{P}_{nm}(\cos\theta)$ is needed to be computed.

We present Eq. (A.1) in the following form

$$
\begin{aligned}
T_{xx} =& \frac{GM}{r^3} \sum_{n=2}^{M} \left(\frac{R}{r} \right)^n \\
& \times \sum_{m=0}^{n} \Bigg[\left(\overline{C}_{n,m+2} \cos(m+2)\lambda + \overline{S}_{n,m+2} \sin(m+2)\lambda \right) a_{n,m+2} \\
& + \left(\overline{C}_{nm} \cos m\lambda + \overline{S}_{nm} \sin m\lambda \right) \left(b_{nm} - (n+1)(n+2) \right) \\
& + \left(\overline{C}_{n,m-2} \cos(m-2)\lambda + \overline{S}_{n,m-2} \sin(m-2)\lambda \right) c_{n,m-2} \Bigg] \\
& \times \overline{P}_{nm}(\cos\theta),
\end{aligned}
\tag{A.9}
$$

where

$$
\left.
\begin{array}{l}
\overline{C}_{n,m+2} \\
\overline{S}_{n,m+2} \\
\cos(m+2)\lambda \\
\sin(m+2)\lambda \\
a_{n,m+2}
\end{array}
\right\} = 0, \quad m+2 > n,
\tag{A.10}
$$

$$
\left.
\begin{array}{l}
\overline{C}_{n,m-2} \\
\overline{S}_{n,m-2} \\
\cos(m-2)\lambda \\
\sin(m-2)\lambda \\
c_{n,m-2}
\end{array}
\right\} = 0, \quad m-2 < 0.
\tag{A.11}
$$

The main idea of Eq. (A.9) is that the set of spherical harmonic coefficients is usually stored during the whole computational process, hence the coefficients $\overline{C}_{n,m+2}, \overline{S}_{n,m+2}$ and $\overline{C}_{n,m-2}, \overline{S}_{n,m-2}$ may be simply restored when necessary instead of the redundant computation of $\overline{P}_{n,m-2}(\cos\theta)$ and

$\overline{P}_{n,m+2}(\cos\theta)$ in Eq. (A.1). The formulae for the remaining elements $T_{yy}, T_{zz}, T_{xy}, T_{xz}, T_{yz}$ may be easily modified in the same way.

References

Barthelmes, F., 2009. Definition of functionals of the geopotential and their calculation from spherical harmonic models. Scientific Technical Report STR09/02. GFZ German Research Centre for Geosciences. Potsdam, Germany, 32pp.

Bethencourt, A., Wang, J., Rizos, C., Kearsley, A.H.W., 2005. Using personal computers in spherical harmonic synthesis of high degree Earth geopotential models, in: Paper presented at Dynamic Planet 2005, Cairns, Australia, 22-26 August 2005.

Bosch, W., 2000. On the computation of derivatives of Legendre functions. Physics and Chemistry of the Earth 25, 655–659.

Colombo, O.L., 1981. Numerical methods for harmonic analysis on the sphere. Report No. 310. Department of Geodetic Science and Surveying, The Ohio State University. Columbus, Ohio, 140pp.

Fantino, E., Casotto, S., 2009. Methods of harmonic synthesis for global geopotential models and their first-, second- and third-order gradients. Journal of Geodesy 83, 595–619. doi: 10.1007/s00190-008-0275-0.

Fukushima, T., 2011. Numerical computation of spherical harmonics of arbitrary degree and order by extending exponent of floating point numbers. Journal of Geodesy 86, 271–285. doi: 10.1007/s00190-011-0519-2.

Fukushima, T., 2012. Numerical computation of spherical harmonics of arbitrary degree and order by extending exponent of floating point numbers: II first-, second-, and third-order derivatives. Journal of Geodesy 86, 1019–1028. doi: 10.1007/s00190-012-0561-8.

Grafarend, E.W., 2006. Linear and Nonlinear Models. Walter de Gruyter, Berlin, New York, 752pp.

Hoffmann-Wellenhof, B., Moritz, H., 2005. Physical Geodesy. Springer, Wien, New York, 403pp.

Holmes, S.A., Featherstone, W.E., 2002a. Extending simplified high-degree synthesis methods to second latitudinal derivatives of geopotential. Journal of Geodesy 76, 447–450. doi: 10.1007/s00190-002-0216-3.

Holmes, S.A., Featherstone, W.E., 2002b. A unified approach to the Clenshaw summation and the recursive computation of very high degree and order normalised associated Legendre functions. Journal of Geodesy 76, 279–299. doi: 10.1007/s00190-002-0216-2.

Holmes, S.A., Pavlis, N.K., 2008. Spherical harmonic synthesis software Harmonic_synth. `http://earth-info.nga.mil/GandG/wgs84/gravitymod/new_egm/new_egm.html`, (accessed 5 December, 2012).

Janák, J., Šprlák, M., 2006. New software for gravity field modelling using spherical harmonics. Geodetic and Cartographic Horizon 52, 1–8 (in Slovak).

Moritz, H., 1980. Advanced Physical Geodesy. Herbert Wichmann Verlag, Karlsruhe, Germany, 500pp.

Moritz, H., 2000. Geodetic reference system 1980. Journal of Geodesy 74, 128–133.

National Imagery and Mapping Agency (NIMA), 2000. World Geodetic System 1984: Its Definition and Relationships with Local Geodetic Systems. Technical Report No. NIMA TR8350.2. National Imagery and Mapping Agency. USA, 175pp.

Pavlis, N.K., Holmes, S.A., Kenyon, S.C., Factor, J.K., 2012. The development and evaluation of the Earth Gravitational Model 2008 (EGM2008). Journal of Geophysical Research 117(B04406), 1–38. doi: 10.1029/2011JB008916.

Pavlis, N.K., K., F.J., Holmes, S.A., 2007. Terrain-related gravimetric quantities computed for the next EGM, in: Proceedings of the 1st International Symposium of the Internationa Gravity Field Service vol. 18, Harita Dergisi, Istanbul, 318-323.

Petrovskaya, M.S., Vershkov, A.N., 2006. Non-singular expressions for the gravity gradients in the local north-oriented and orbital reference frames. Journal of Geodesy 80, 117–127. doi: 10.1007/s00190-006-0031-2.

Rektorys, K., 1999. Variational Methods in Engineering and in Mathematical Physics. Academia, Prague, 602pp (in Czech). 2nd edition.

Sanso, F., Sona, G., 2001. ELGRAM: an Ellipsoidal Gravity Model Manipulator. Bollettino di Geodesia e Scienze Affini 60, 3, 215–226.

Smith, D.A., 1998. There is no Such Thing as "The" EGM96 Geoid: Subtle Points on the Use of a Global Geopotetial Model. IGeS Bulletin 8, 17–28.

554 Smith, J.M., Olver, F.W.J., Lozier, D.W., 1981. Extended-range arithmetic
555 and normalized Legendre polynomials. ACM Trans Math Softw 7, 93–105.

556 Tscherning, C.C., Rapp, R.H., Goad, C., 1983. A comparision of methods
557 for computing gravimetric quantities from high degree spherical harmonic
558 expansions. Manuscripta Geodaetica 8, 249–272.

559 Wittwer, T., Klees, R., Seitz, K., Heck, B., 2008. Ultra-high degree spherical
560 harmonic analysis and synthesis using extended-range arithmetic. Journal
561 of Geodesy 82, 223–229. doi: 10.1007/s00190-007-0172-y.

List of Tables

List of Figures

Table A.1: Structure of the input GGM file – spherical harmonic coefficients sorted primarily according to degrees.

n	m	$\overline{C}_{nm}$	$\overline{S}_{nm}$
2	0	-0.48417E-03	0.00000E+00
2	1	-0.20662E-09	0.13844E-08
2	2	0.24394E-05	-0.14003E-05
3	0	0.95716E-06	0.00000E+00

Table A.2: Structure of the input GGM file – spherical harmonic coefficients sorted primarily according to orders.

n	m	$\overline{C}_{nm}$	$\overline{S}_{nm}$
2	0	-0.48417E-03	0.00000E+00
3	0	0.95712E-06	0.00000E+00
4	0	0.53998E-06	0.00000E+00
5	0	0.68658E-07	0.00000E+00

Table A.3: Structure of the input file of error variance-covariance matrix – spherical harmonic coefficients sorted primarily according to orders; $n_{\min} = 2$; $n_{\max} = 3$; the column CS determines whether the variance and covariances in the particular line are related to the coefficient $\overline{C}_{nm}$ (if $CS = 0$) or to the coefficient $\overline{S}_{nm}$ (if $CS = 1$).

CS	n	m	variances and covariances of the spherical harmonic coefficients
0	2	0	4.31E-25
0	3	0	-2.11E-26 2.48E-25
0	2	1	3.79E-28-1.15E-27 3.84E-25
1	2	1	-3.44E-28 4.67E-28-1.17E-27 4.16E-25
0	3	1	1.99E-27-7.61E-29 2.98E-26-3.18E-28 2.48E-25
1	3	1	1.44E-28-8.80E-29 3.42E-28 2.54E-26-3.16E-27 2.70E-25
0	2	2	8.17E-27-1.72E-27 2.94E-28 3.67E-28 9.06E-29-1.08E-27 4.02E-25
1	2	2	1.14E-27 2.94E-28-5.61E-29-3.86E-28-1.23E-27-1.50E-27 8.37E-28 4.25E-25
0	3	2	-9.38E-27 6.35E-27 1.08E-27 1.81E-27 7.12E-28 3.53E-28 3.30E-26 9.75E-29 3.07E-25
1	3	2	-1.27E-28 3.45E-27 1.59E-27 7.97E-28-1.75E-28 1.15E-28 5.51E-28 2.30E-26 2.78E-27 3.09E-25
0	3	3	7.74E-28-1.36E-28-9.93E-27 5.50E-28 9.55E-28-3.25E-27 1.06E-27-8.60E-28-2.85E-29 1.58E-28 2.74E-25
1	3	3	-1.14E-27-2.19E-28 4.51E-28-1.26E-26-1.46E-28 4.90E-27 1.25E-28-1.76E-28 1.18E-28-5.22E-29-6.97E-29 2.74E-25

Table A.4: Demonstration of the report file created by the GrafLab.

Software	GrafLab 1.00
Generating date	28-Oct-2012
Generating time	13:46:13
Computed	Functionals of the geopotential
Geopotential model file	go_cons_gcf_2_dir_r1.dat
GM of the geopotential model ($m^3 \cdot s^{-2}$)	3.986004415e+014
R of the geopotential model (m)	6.378136460e+006
Minimum used degree	2
Maximum used degree	240
Reference ellipsoid	GRS80
Latitude limit North (deg)	90.000000000
Latitude limit South (deg)	-90.000000000
Longitude limit West (deg)	0.000000000
Longitude limit East (deg)	360.000000000
Latitude parallels	1801
Longitude parallels	3601
Number of grid points	6485401
Grid height above the ellipsoid (m)	0.000
Computation time (s)	4
Computation of fully normalized ALFs	Standard forward column method

Exported data file contains the following columns:

Latitude (deg) Longitude (deg) Disturbing_potential ($m^2 \cdot s^{-2}$)

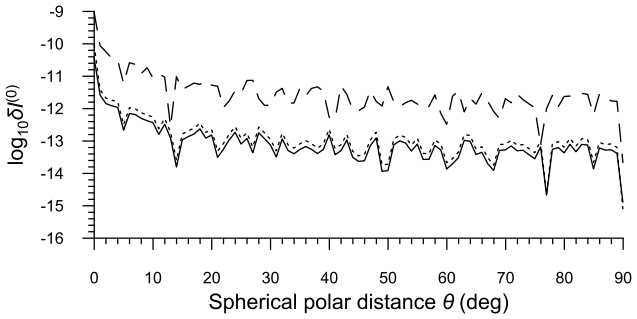

Figure A.1: Base-10 logarithm of the identity error $\delta I^{(0)}$ of fnALFs using: (i) the standard forward column method (maximum degree: $M = 1\ 800$; *solid line*); (ii) the modified forward column method (maximum degree: $M = 2\ 700$; *dotted line*); (iii) the extended-range arithmetic (maximum degree: $M = 65\ 536$; *dashed line*).

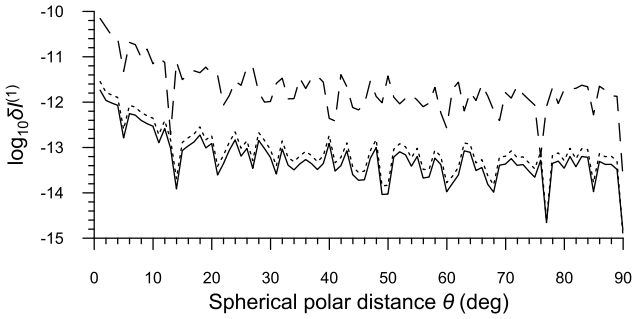

Figure A.2: Base-10 logarithm of the identity error $\delta I^{(1)}$ of the first-order derivatives of fnALFs using: (i) the standard forward column method (maximum degree: $M = 1\ 800$; *solid line*); (ii) the modified forward column method (maximum degree: $M = 2\ 700$; *dotted line*); (iii) the extended-range arithmetic (maximum degree: $M = 65\ 536$; *dashed line*).

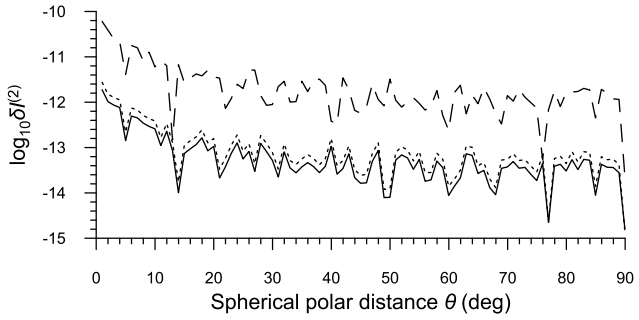

Figure A.3: Base-10 logarithm of the identity error $\delta I^{(2)}$ of the second-order derivatives of fnALFs using: (i) the standard forward column method (maximum degree: $M = 1\,800$; *solid line*); (ii) the modified forward column method (maximum degree: $M = 2\,700$; *dotted line*); (iii) the extended-range arithmetic (maximum degree: $M = 65\,536$; *dashed line*).

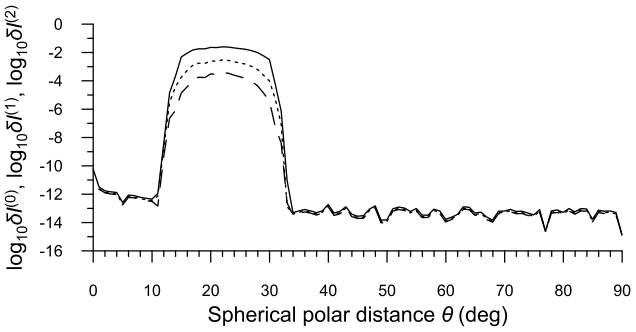

Figure A.4: Base-10 logarithm of the identity errors $\delta I^{(0)}$, $\delta I^{(1)}$, $\delta I^{(2)}$ of the zero-, first- and second-order derivatives of fnALFs, respectively, using the standard forward column method (maximum degree: $M = 2\,190$; $\delta I^{(0)}$ – *solid line*; $\delta I^{(1)}$ – *dotted line*; $\delta I^{(2)}$ – *dashed line*).

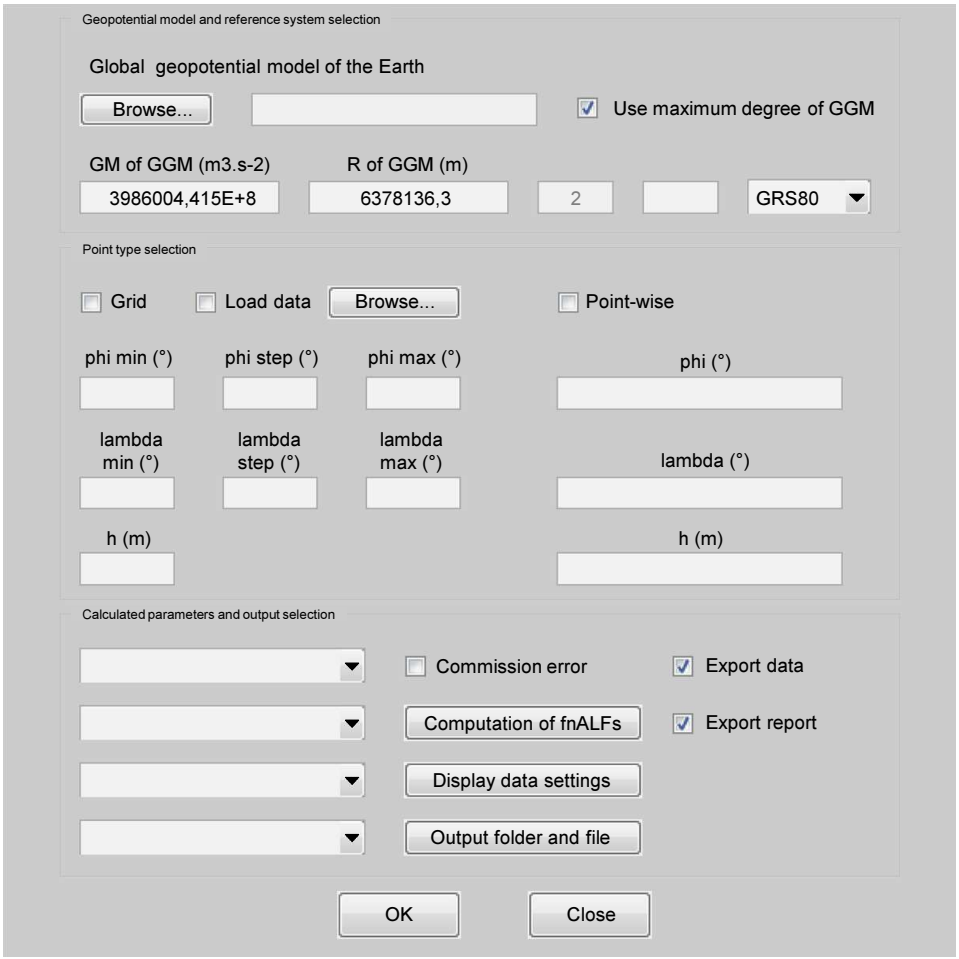

Figure A.5: GrafLab graphical user interface.

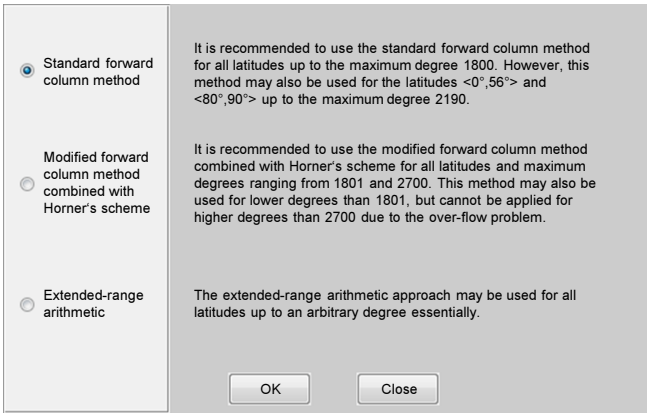

Figure A.6: Computation of fnALFs window.

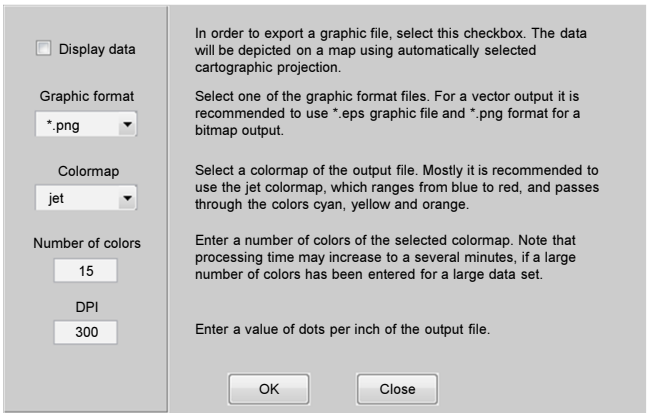

Figure A.7: Display data settings window.

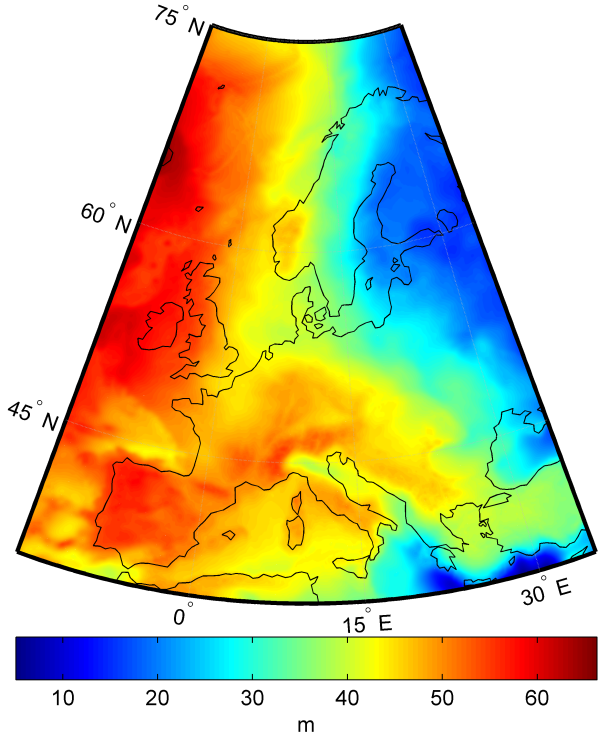

Figure A.8: Geoid undulation computed and depicted using the GrafLab software. The geoid undulation is computed on the regular grid $\varphi \in \langle 35°, 75° \rangle$, $\lambda \in \langle -15°, 35° \rangle$ with spatial resolution 0.1° using EGM2008 and DTM2006.0 (maximum degree of SHE: $M = 2\,190$).

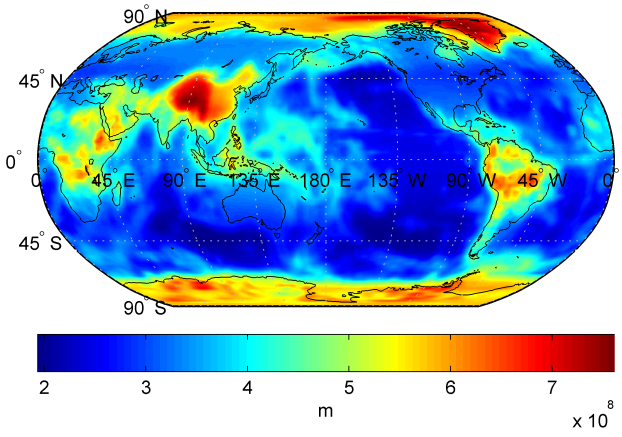

Figure A.9: Commission error of geoid undulation computed and depicted using the GrafLab software. The commission errors of geoid undulation are computed on the regular grid $\varphi \in \langle -90°, 90° \rangle$, $\lambda \in \langle 0°, 360° \rangle$ with spatial resolution $2°$ using the full error variance-covariance matrix of GRIM5C1 (maximum degree of SHE: $M = 70$; the error variance-covariance matrix is not calibrated).

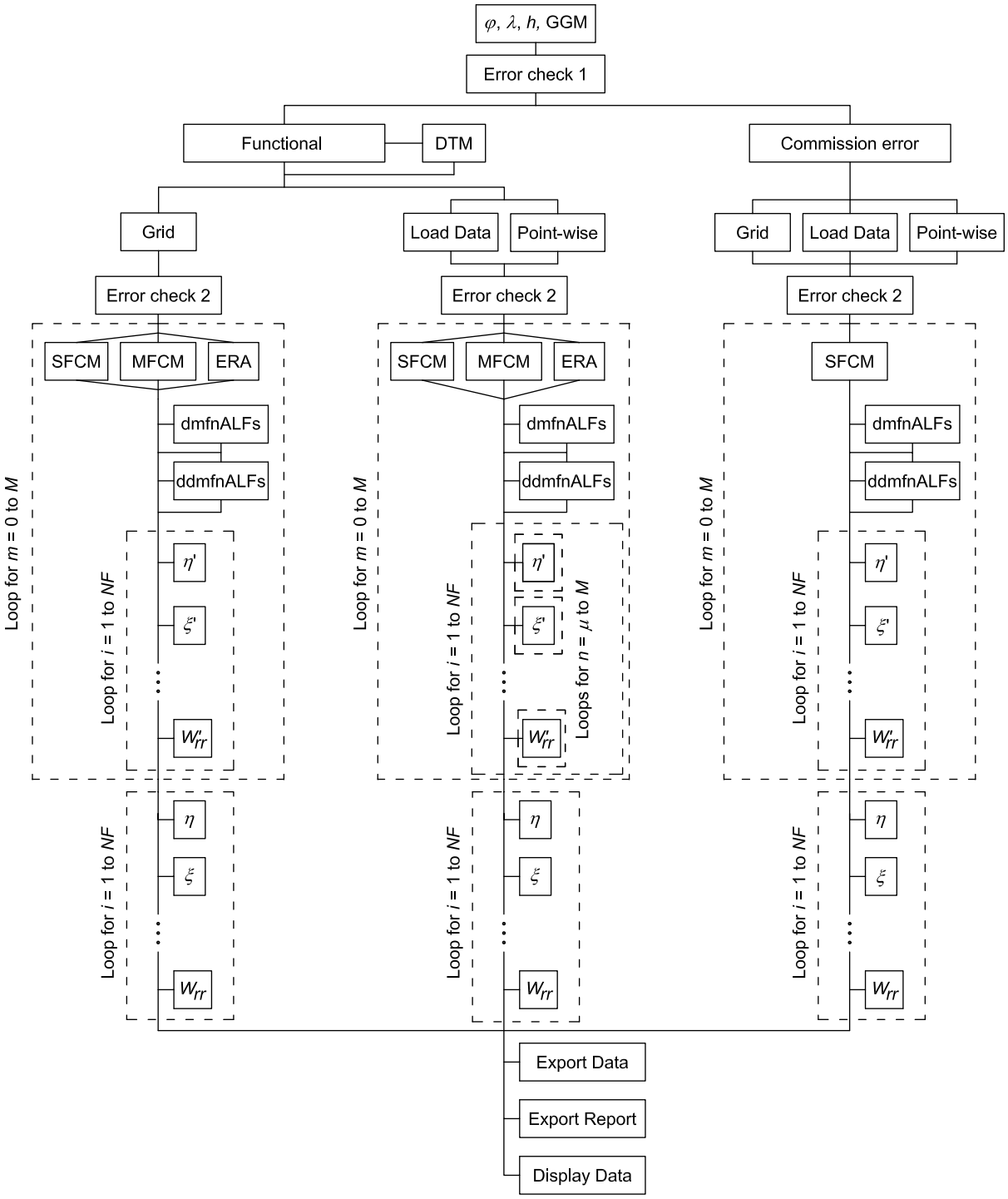

Figure A.10: Flowchart of the GrafLab. Explanation of the symbols and abbreviations in the flowchart: φ, λ, h, GGM – ellipsoidal coordinates of the evaluation points, global geopotential model of the Earth; Error check 1 – the first error check of the input data; DTM – digital terrain model; Error check 2 – the second error check of the input data; Grid, Load data, Point-wise – point type selection; SFCM, MFCM, ERA – computation of the fnALFs using the standard forward column method, the modified forward column method

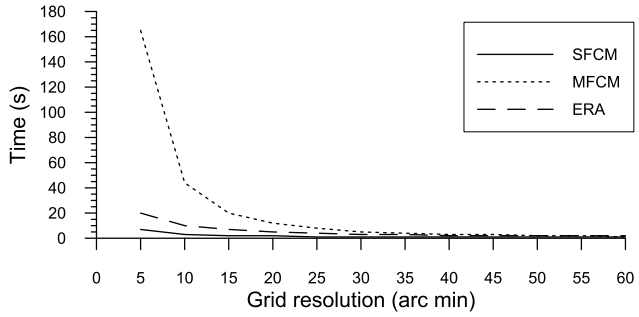

Figure A.11: CPU time for synthesis of disturbing potential using $M = 360$ versus grid resolution (SFCM - standard forward column method; MFCM - modified forward column method; ERA - extended-range arithmetic).

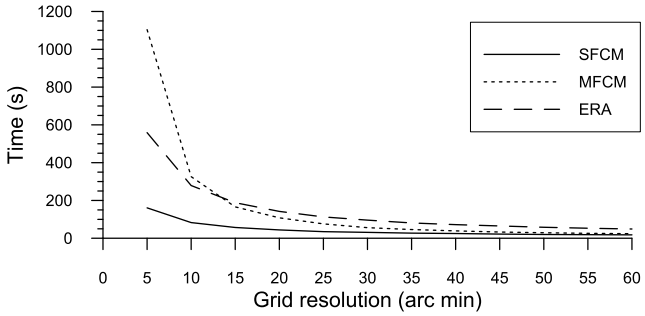

Figure A.12: CPU time for synthesis of disturbing potential using $M = 2\ 190$ versus grid resolution (SFCM - standard forward column method; MFCM - modified forward column method; ERA - extended-range arithmetic).

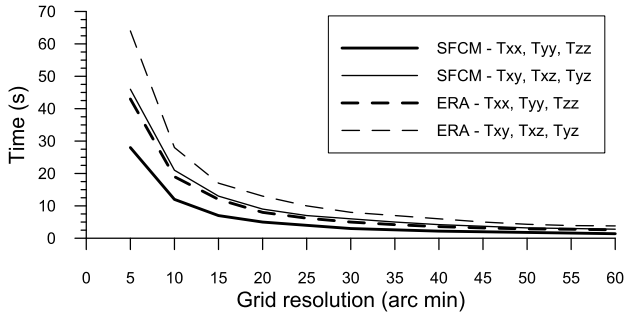

Figure A.13: CPU time for synthesis of disturbing tensor using $M = 360$ versus grid resolution (SFCM - standard forward column method; ERA - extended-range arithmetic).

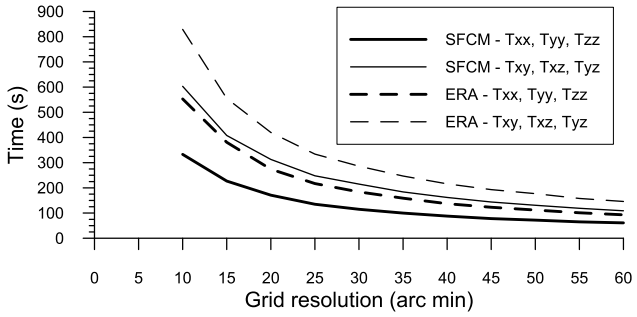

Figure A.14: CPU time for synthesis of disturbing tensor using $M = 2\ 190$ versus grid resolution (SFCM - standard forward column method; ERA - extended-range arithmetic).

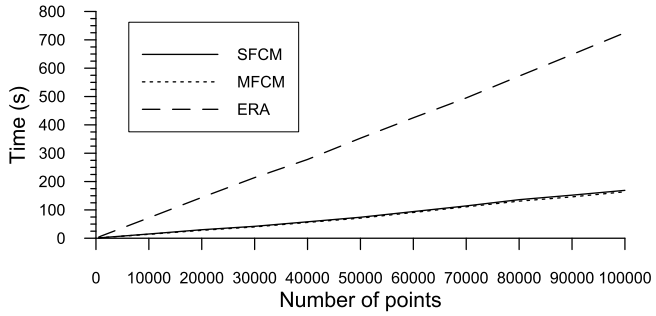

Figure A.15: CPU time for synthesis of disturbing potential using $M = 360$ versus number of points (SFCM - standard forward column method; MFCM - modified forward column method; ERA - extended-range arithmetic).

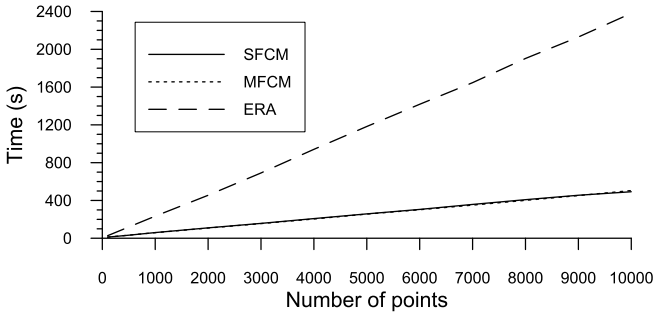

Figure A.16: CPU time for synthesis of disturbing potential using $M = 2\ 190$ versus number of points (SFCM - standard forward column method; MFCM - modified forward column method; ERA - extended-range arithmetic).

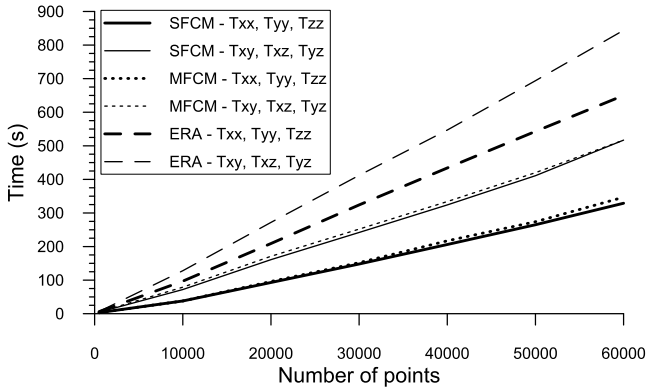

Figure A.17: CPU time for synthesis of disturbing tensor using $M = 360$ versus number of points (SFCM - standard forward column method; MFCM - modified forward column method; ERA - extended-range arithmetic).

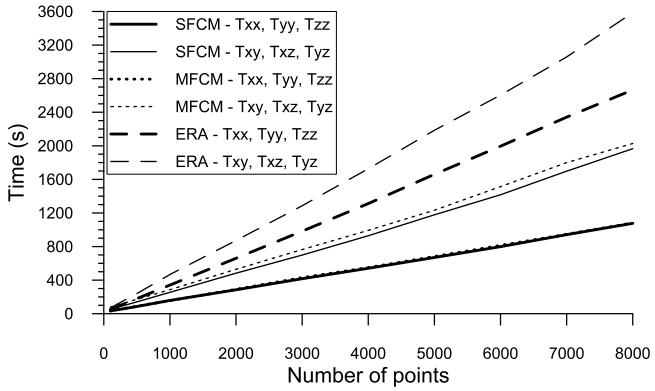

Figure A.18: CPU time for synthesis of disturbing tensor using $M = 2\ 190$ versus number of points (SFCM - standard forward column method; MFCM - modified forward column method; ERA - extended-range arithmetic).